Int J Thermophys (2009) 30:1074–1087
DOI 10.1007/s10765-009-0614-2

Thermal Degradation Studies of Polythiophenes Containing Hetero Aromatic Side Chains

S. Radhakrishnan · N. Somanathan · M. Thelakkat

Received: 20 July 2007 / Accepted: 17 June 2009 / Published online: 7 July 2009

Abstract Thiophene monomer structures containing different hetero aromatic rings (containing five-member/six-member, varying electronegativity, functional groups) were designed and synthesized. The influence of structural components of the side chain on the thermal stability of the polymers of the above monomers was analyzed using thermogravimetric analysis. The results show that thiophene-containing hetero aromatic side chains linked through six-member ring show high thermal stability.

Keywords Hetero aromatic · Polythiophene · Thermal stability · Thermogravimetry

1 Introduction

Polymers are useful materials as a result of their ease of fabrication, flexibility, lightness of weight, and chemical inertness. As such, electrically conducting polymers are potential candidates for a wide variety of applications ranging from electrode materials and microelectronic devices to electrochromic display devices. Because of that, conjugated polymers are the subject of study, where a wide variety of polyenes, polyaromatics, and polyheterocycles were investigated in the search for conducting polymers with improved properties. Polythiophene (PT) and its soluble derivatives occupy a special role in the development of conjugated polymers as electrically conductive and optoelectronic materials because of their stability in both neutral and doped states, their high electrical conductivity and their interesting electronic and optical properties.

S. Radhakrishnan · N. Somanathan (✉)
Polymer laboratory, Central Leather Research Institute, Chennai 600 020, India
e-mail: nsomanathan@rediffmail.com

M. Thelakkat
Macromolecular Chemistry I, University of Bayreuth, Bayreuth 95447, Germany

One of the advantages of PTs is the ease of tailoring electronic and optical properties by attaching different functional groups at the 3- and/or 4-positions of the thiophene ring and/or by controlling the regularity of the backbone through synthetic methodology. Electroluminescent emission from blue to near infrared has been achieved from PTs by attaching sterically hindered substituents at different positions of the chain.

Insertion of azomethine moieties (Schiff bases) in the backbone of conjugated polymers have been shown to be useful for the preparation of materials with high molar mass and good physico-mechanical properties. Destri et al. [1] reported on the synthesis of a series of polymers comprising alternating sequences of thienylene and phenylene residues linked together by azomethine moieties. Ng et al. [2] studied structure–properties relations by incorporating thienylenic or furanylenic and phenylene residues linked together with azomethine moieties. It was shown that the above compounds exhibit high thermal stability. Polymers containing thiophene moiety show higher thermal stability since the sulphur atom in the thiophene ring is less able to donate electrons, thus stabilizing free radicals formed during thermal oxidation.

Organic light emitting diodes (OLEDs) represent a new basis for light emissive flat panel displays. The luminosity of OLEDs is due to the recombination of excitons near the organic–organic hetero interface. At present, the OLED lifetime is one of the primary issues limiting the widespread commercial use of these devices; consequently an understanding of their degradation mechanism is of broad interest [3]. These include electrode reactions that destroy the polymer–metal interface and photo-oxidation of the emissive polymer. Thermally induced strain resulting in device failure has also been observed for OLEDs [4]. In LEDs, much of the electrical energy has been transformed into heat apart from optical energy conversion. This instantaneous heat developed on the materials may bring defects at the interface of the layers apart from thermal degradation, which may modify the conductivity and change the device characteristics, which may ultimately lead to device failure. Therefore, the thermal stability of the photo-emissive polymers is important to get good device efficiency and long lifetime.

Functional groups and the nature of the side chain influence the thermal stability of the substituted PTs. Glass transition temperature (T_g) and thermal stability of phenylene functionalized PTs decrease with an increase in the side chain length [5]. Due to this, the onset of thermal degradation was shifted above 300 °C. The same trend is observed in 3-alkoxy substituted thiophene [6]. In the above compounds, complete decomposition temperature of polymers increases with increasing pendent chain length, probably attributed to the occurrence of cross-linking in polymers with a longer side chain during a T_g scan [7]. Herrera and Whitten [8] reported that the presence of a urethane side chain in PTs broadens the π-conjugated features to such an extent that they cannot be resolved until the side chain decomposes. The urethane side chain decomposition takes place between 250 °C and 300 °C, while the thiophene backbone is stable at temperatures well above 400 °C in the above-mentioned thiophene compounds containing urethane linkage.

In the present investigation, the thermal stability of thiophene polymers containing hetero aromatic rings (side chains containing nitrogen and sulphur in the aromatic ring) linked through azomethine groups is studied. The synthesized structures included in the present study are shown in Fig. 1. The designed structures are organized in

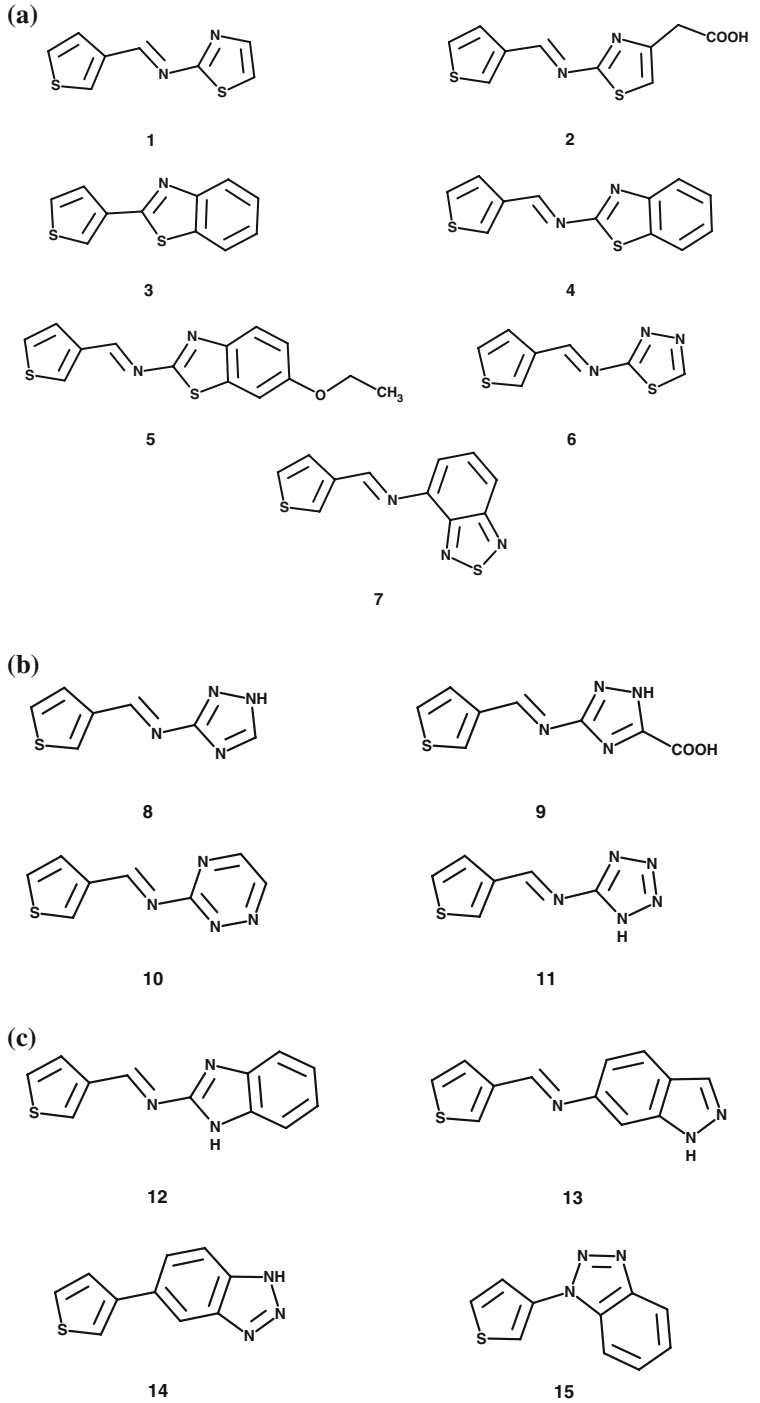

Fig. 1 Different chemical structures of polymers: (**a**) Group 1, (**b**) Group 2, and (**c**) Group 3

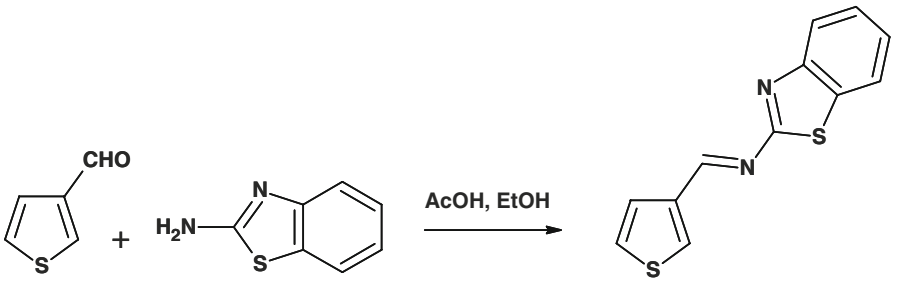

Scheme 1 Synthesis of thiophene-3-imines

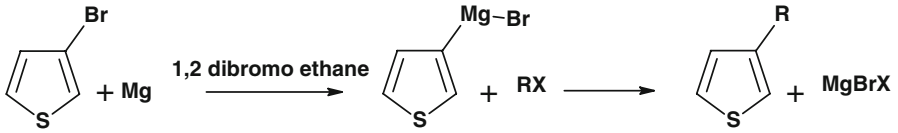

Scheme 2 Synthesis of 3-(aryl) thiophene

three groups. The first group consists of thiophene compounds substituted with a five-member ring containing sulphur and nitrogen at different positions. The second group is designed with structures containing a different number of nitrogen atoms in the heterocyclic ring (two to four nitrogen atoms). Similarly, the third group consists of structures containing phenyl ring fused hetero cyclics, especially based on imidazoles, indazoles, and triazoles.

2 Experimental

2.1 General Method of Preparation of Imines

The corresponding amines, dissolved in ethanol, were reacted with thiophene-3-carboxaldehyde in the presence of a catalytic amount of acetic acid. The mixture was refluxed for an hour, and the resulting solid was filtered and washed with ethanol. The compound was purified by recrystallization. Monomers of compounds like **1**, **2**, **4**, **5**, **6**, **7**, **8**, **9**, **10**, **11**, **12**, and **13** were synthesized by using the general procedure in Scheme 1.

2.2 General Method of Preparation of 3-(aryl) Thiophene

A Grignard compound of 3-bromothiophene was prepared by reacting it with magnesium using 1,2-dibromo ethane as an entrainer in dry diethyl ether medium, and it was coupled with a 2-chloro compound of the heterocyclic compound in the presence of nickel catalyst. The resulting materials were purified by column chromatography.

A monomer of **3** was synthesized as shown in Scheme 2, and the experimental procedure followed for the synthesis is as follows.

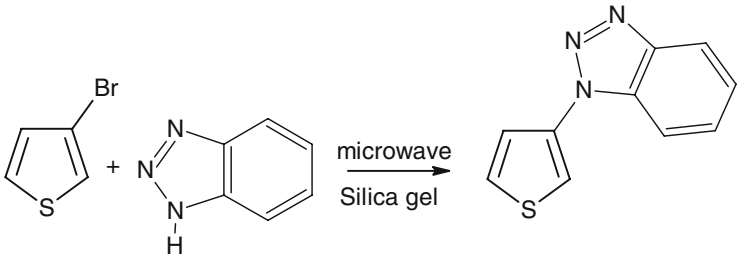

Scheme 3 Microwave synthesis of 3-(aryl) thiophene

3-bromo thiophene (0.01 mol) and magnesium turnings (0.01 mol) were introduced together with dry diethyl ether in a three-necked flask fitted with a condenser, a dropping funnel, and a nitrogen inlet. The entrainer 1,2-dibromo ethane (0.01 mol) in anhydrous diethyl ether was then added at ice-cold temperature for a period of 8 h. After the reaction began, the solution was brought to ambient temperature. The resulting Grignard compound was transferred to a second dropping funnel fitted to a second three-necked flask containing 2-chloro benzothiazole (0.01 mol) and 1,3-bis (diphenyl phosphino propane) nickel (II) chloride (Nidppp) in anhydrous diethyl ether. After cooling with an ice bath, the Grignard compound was added drop wise and the resulting adduct was allowed to warm to ambient temperature and was stirred for 1 h before being refluxed for 24 h. The obtained mixture was poured onto very dilute aqueous hydrochloric acid. The organic layer was washed with water, dried, and concentrated. The crude product was purified on a silica gel column using petroleum ether (boiling range 60 °C to 80 °C) as an eluent. A similar procedure was adopted for the synthesis of the **14** monomer.

2.3 Microwave Assisted Synthesis of Monomer **15**

Monomer **15** was synthesized by the reaction shown in Scheme 3 using microwave synthesis and the procedure followed for the synthesis is as follows. 0.01 mol of 1H-benzotriazole was dissolved in 5 ml of chloroform. 0.01 mol of 3-bromothiophene was added to the above solution and chloroform solution was adsorbed in 20 g of silica gel (60 to 120 mesh). The silica gel was dried and subjected to microwave irradiation for 5 min. The maximum time of reaction and microwave dosage were fixed on the basis of the study of kinetics of the reaction. The obtained product was extracted with chloroform and further treated with 1 % dilute hydrochloric acid to remove the unreacted amine. The organic layer was washed with water, dried over anhydrous sodium sulphate, and purified further with column chromatography.

2.4 General Method of Preparation of Polymers by Electrochemical Polymerization

The electrochemical polymerizations of Schiff's bases were carried out in acetonitrile containing tetrabutylammonium hexafluorophosphate ($TBAPF_6$) as the electrolyte.

The current density for the polymerization reaction was $1.43\,\mathrm{mA}\cdot\mathrm{cm}^{-2}$, and the reaction was performed for 4 h with the above current density. Dedoping of the formed polymers was carried out for 30 min by reversing the polarity. The time of reaction and dedoping were fixed on the basis of the applied current. The above procedure was adopted for synthesizing all polymers.

The thermal stability of the polymers was studied in nitrogen with thermogravimetric analysis using a Netstch 609 thermal analyzer with a heating rate of $10\,^{\circ}\mathrm{C}\cdot\mathrm{min}^{-1}$.

3 Results and Discussion

In this study, the thermal stability of the compounds is monitored using thermogravimetry and the obtained results are used to compare the thermal stability of different structures of thiophene polymers. The thermograms obtained for different compounds of Groups 1, 2, and 3 are, respectively, presented in Fig. 2a, b, and c.

Even though the selection of emissive materials for LEDs primely depend on fluorescence and electroluminescence (EL) characters, other properties like thermal stability are also important. This is due to the fact that in LEDs, the EL conversion efficiency is around 5 % and the remaining electrical energy may dissipate in the form of heat as mentioned earlier. This thermal energy instantaneously raises the temperature of the emissive layer. Therefore, for PLED applications, it is mandatory that the polymer should also have good thermal stability. To understand the stability of the compounds at specific temperatures, the degrees of degradation at 473 K, 573 K, 673 K, and 773 K are compared (Table 1). At 573 K, **10P** has very high thermal stability compared to other compounds. **2P** and **13P** also have better thermal stability than other polymers at the above temperature (573 K). **10P** shows a very high degradation rate between 573 K and 673 K, and it completely degrades. Similarly, **9P** shows poor thermal stability. Polymers of structures like **2P**, **13P**, **14P**, and **15P** show very high thermal stability even at high temperatures (773 K).

To understand the kinetics of degradation at different degradation stages, a logarithmic relation of concentration is plotted against the inverse of temperature ($1/T$). At every stage of degradation, the percentage mass loss is computed (Table 2). The activation energy for the different stages of degradation is calculated for the different polymers using the Doyle equation [9],

$$\ln(1-C) = -2.315(A/B) + 0.4567(A/B)(E/R)(1/T) \tag{1}$$

where C is the fractional mass loss, $1-C$ is the fractional mass remaining after a sample is heated to a temperature T; R is the universal gas constant; and A and B are constants. The activation energy is calculated from the slope obtained from the plot of $\ln(1-C)$ against $(1{,}000/T)$. The representative relation obtained for 1P is shown in Fig. 3. The tangent to the slope of the $\ln(1-C)$ versus $1/T$ plot over various intervals of the data was used to interpret the complicated decomposition of the polymers, and these tangents were used to calculate the effective activation energies at these temperature regimes. The calculated activation energy for different degradation stages is presented in Table 2.

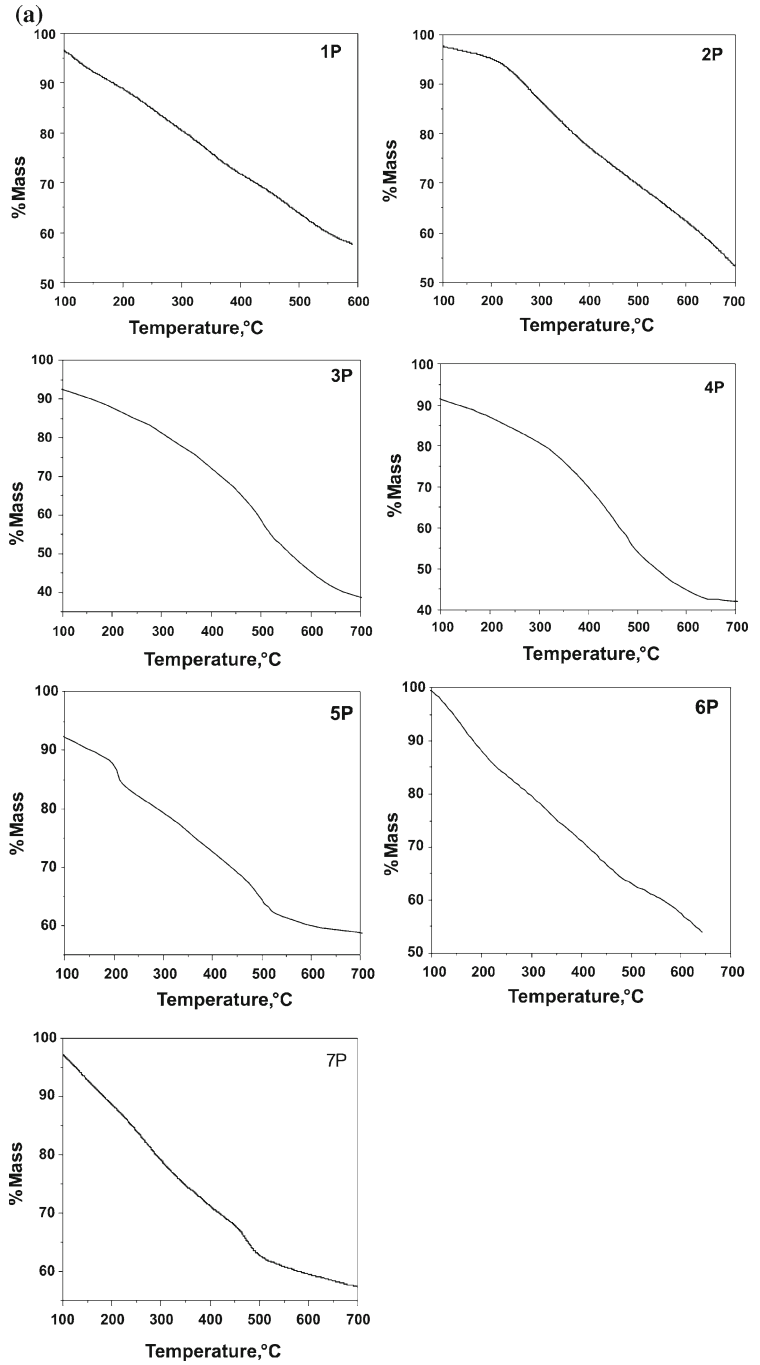

Fig. 2 Thermograms of different polymers: (**a**) Group 1, (**b**) Group 2, and (**c**) Group 3

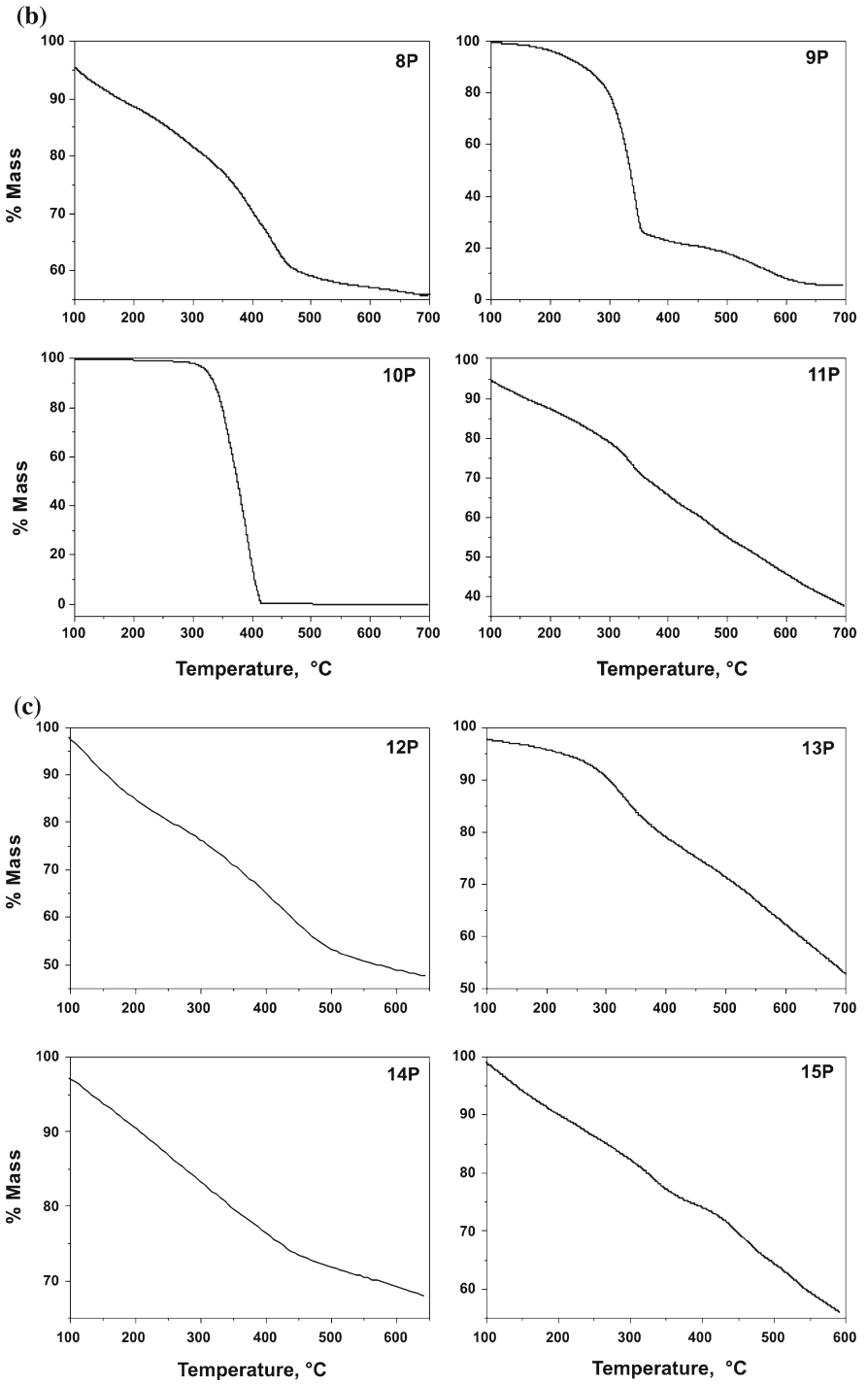

Fig. 2 continued

Table 1 Effect of structure on thermal degradation at different temperatures for Groups 1, 2, and 3

Polymer	% Degradation at			
	473 K	573 K	673 K	773 K
1	11.14	19.47	28.19	36.10
2	4.82	13.25	22.60	30.15
3	12.45	18.60	27.91	41.86
4	13.18	18.60	27.91	41.86
5	12.40	20.93	27.91	35.66
6	12.16	20.57	28.97	36.80
7	11.37	20.94	28.79	37.19
8	11.13	18.09	29.30	40.71
9	3.50	20.32	77.25	82.14
10	0.57	1.95	84.35	99.81
11	12.19	20.50	33.95	44.48
12	15.11	23.43	34.98	46.54
13	3.99	9.40	20.82	28.48
14	9.54	16.79	23.51	28.15
15	9.84	17.71	25.91	35.56

From Table 1, it is evident that the major loss of mass is obtained between 573 K and 673 K in all compounds. As supported by the thermal data, the nitrogen-containing fused heterocycle ring substituted thiophene (**14P** and **15P**) and thiazole-containing **2P** have high thermal stability. Overall studies on polythiophene bearing more electron deficient side chains show high efficiency in photo- and electro-emission apart from having high thermal stability. The side chains of these thiophene structures help to enhance electron transport apart from enhancing emission intensity and covering the emission in the base color range. To get further insights on the influence of polymer structure on thermal stability, thermal data of compounds of similar structures are compared.

3.1 Comparison of **1P** and **2P**

Comparison of the thermal data of polymers of **2P** and **1P** indicate the influence of the acetic acid group, which increases the thermal stability. In the first region of degradation (347 K to 500 K) 14.5 $kJ \cdot mol^{-1}$ is spent for a mass loss of 11.66 % of **1P**, while 13.4 $kJ \cdot mol^{-1}$ is spent to degrade 3.6 % of **2P**. Similarly, in the 500 K to 599 K temperature region, 17.2 $kJ \cdot mol^{-1}$ is needed to degrade 7.62 % of **1P**, while 19.96 $kJ \cdot mol^{-1}$ of energy is spent for degrading 9.58 % of **2P**. These effects can be attributed to the influence of the aliphatic segment present in the 4-position of the thiazole ring. In general, the extension of conjugation aids in the formation of free radicals and decreases the thermal stability.

Table 2 Energy of activation (in $kJ \cdot mol^{-1}$) and percent mass loss for different thermal degradation ranges

Polymer	Temp (K)	Mass loss (%)	E_a ($kJ \cdot mol^{-1}$)
(a) Group 1			
1	347–500	11.66	14.50
	500–589	7.62	17.19
	589–725	11.19	19.23
	725–863	10.21	22.53
2	385–500	3.60	13.38
	500–599	9.58	19.96
	599–855	20.44	20.82
	855–971	10.28	27.80
3	352–503	7.80	12.09
	503–698	16.98	16.33
	698–938	28.95	26.04
4	345–440	4.42	10.80
	440–634	10.32	14.13
	634–903	35.24	24.23
5	466–489	3.61	17.10
	489–687	12.79	14.94
	687–811	10.10	23.79
6	385–630	23.73	16.20
	630–734	8.84	20.70
	734–851	6.86	19.02
	851–916	5.06	25.50
7	369–516	12.75	15.41
	516–725	17.01	18.19
	725–769	4.68	23.49
	769–972	5.68	15.00
(b) Group 2			
8	343–521	12.55	13.97
	521–637	9.98	17.81
	637–748	15.64	23.64
	748–972	4.50	10.34
9	338–478	3.65	13.94
	478–595	31.26	20.92
	595–633	39.32	24.69
	633–681	3.28	15.62
	681–794	6.23	14.02
	794–901	9.60	28.48
	901–970	1.11	15.12
10	361–380	0.24	15.19
	380–537	0.75	13.71
	537–625	21.72	21.66

Table 2 continued

Polymer	Temp (K)	Mass loss (%)	E_a (kJ · mol^{-1})
	625–680	60.08	27.13
	680–691	6.53	28.54
	691–798	0.64	18.53
11	345–559	16.80	14.08
	559–789	26.74	20.70
	789–972	15.85	25.44
(c) Group 3			
12	370–629	27.68	15.45
	629–781	17.51	22.32
	781–917	5.24	17.13
13	357–549	5.62	12.81
	549–641	10.78	21.98
	641–800	12.83	21.76
	800–1014	20.48	27.80
	1014–1173	17.70	35.71
14	335–447	7.38	14.24
	447–552	7.50	16.58
	552–741	11.92	18.19
	741–916	4.79	18.68
15	370–559	15.65	15.72
	559–633	7.14	19.91
	633–699	4.05	17.32
	699–863	16.26	24.01

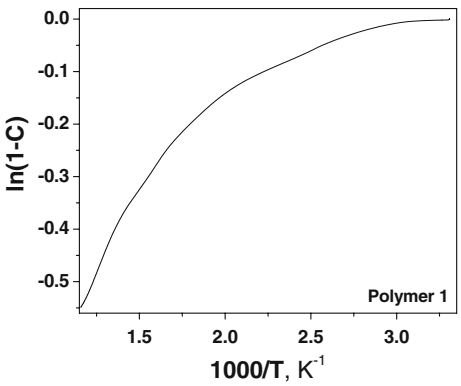

Fig. 3 Plot of $\ln(1 - C)$ versus $1/T$ obtained for Polymer 1 (**1P**)

3.2 Comparison of **1P** and **4P**

In the lower temperature transition region, due to the influence of the fused six-member ring, the stability goes up. Due to this, the energy needed for the degradation

is always higher in **4P** than in **1P**. In general, the five-member thiazole ring feels more strain and therefore thermal stability is affected as in the case of **1P**.

3.3 Comparison of **3P** and **4P**

Linking of the benzothiazole ring attached to the three position of thiophene not only increases the band gap (blue shift) but also the thermal stability. Comparison of **3P** and **4P** clearly shows that, due to the incorporation of azomethine linkage, the energy of degradation of **4P** (first range) is less by about 13.18 %, while 12.45 % of **3P** was degraded at 475 K and it takes higher energy for degradation. In the higher temperature ranges, **4P** takes less energy for degradation than **3P**.

3.4 Comparison of **4P** and **5P**

The presence of the ethoxy group at the six-position of the benzothiazole ring brings more thermal stability as seen from the second stage of degradation.

3.5 Comparison of **6P** and **7P**

In **6P**, the first stage of degradation is extended to 630 K due to the influence of the fused phenyl ring attached to thiadiazole. The results also reveal that the linkage of the hetero aromatic ring influences the degradation. Even though the temperature of the first stage of degradation was extended to higher temperature, the mass loss of **6P** over **7P** does not show any characteristic variation. The energy of activation for 369 K to 725 K range for **7P** is lower than the values obtained for **6P**, suggesting that **6P** is more stable than **7P**.

3.6 Comparison of **8P** and **9P**

The overall results suggest that **8P** has higher stability than **9P**. **8P** degrades in three stages while **9P** loses its mass by 7-stage degradation. At 773 K, **9P** has lost 82 % of its initial mass. It may be due to the presence of carboxylic acid at the five-position of the triazole ring, which aids the possible rearrangement of the ring with the removal of nitrogen. At the first stage (at 447 K), **9P** is more stable than **8P**. Major degradation occurs in **9P** between 573 K and 673 K. Between 478 K and 595 K, **9P** loses 31 %, and about 39 % is lost between the temperature ranges of 595 K and 633 K. In contrast to this, **8P** loses only 10 % and 15 %, respectively, in the temperature ranges of 521 K to 637 K and 637 K to 748 K. The very high mass loss observed in **9P** is due to the –COOH group attached to the five-position of the ring.

3.7 Comparison of **8P** and **11P**

Comparison of the thermal degradation results obtained for **8P** and **11P** show that due to the presence of more electronegative nitrogen, the thermal stability of **11P** is reduced. **8P** degrades by a four-stage process, while in **11P**, the degradation takes

place in three stages. In the first stage of degradation, even though the temperature range and energy of activation are comparable, the mass loss is 25 % higher in the case of **11P** when compared to **8P**, which can be due to the presence of four nitrogens in the ring.

Comparison of the third stage of degradation (748 K to 922 K) of **11P** and **8P** show that the thermal degradation of **11P** was very much influenced by the presence of four nitrogens and about 15.85 % was lost with the very high activation energy of $25.44\,\mathrm{kJ}\cdot\mathrm{mol}^{-1}$. The overall results clearly indicate that the presence of the tetrazole ring reduces the thermal stability compared to the polythiophene containing triazole.

3.8 Comparison of **8P** and **10P**

To understand the influence of the presence of five-member and six-member rings on thermal stability, the activation energy and mass loss of **8P** and **10P** are compared. **10P** is expected to be more aromatic and have more extended conjugation than **8P**. In initial stages (573 K), **10P** does not show any degradation and has very high thermal stability, while **8P** lost about 18 % of its original mass. Major degradation occurs in **10P**, and 60 % of its mass was lost between 625 K and 680 K. The overall results clearly indicate that the extended conjugation in triazine aids in the degradation. It is interesting to note that the above results have a similar trend to the high degradation in **9P**, which is aided by the presence of –COOH at the five-position allowing for extended conjugation.

3.9 Effect of Linkage on Thermal Degradation

3.9.1 Comparison of **12P** *and* **13P**

The thermal data obtained for **12P** and **13P** are compared in order to understand the influence of linkage of the hetero aromatic ring to thiophene. In **12P**, the benzimidazole ring is attached to thiophene through the five-member ring while it is linked through the six-member ring in **13P**. The strain imparted by the five-member ring is much higher than that from the six-member ring as mentioned earlier. It is interesting to note that the above effect really influences the thermal stability, and at all temperatures under study, the mass loss is higher in **12P** than in **13P**. In the first stage of degradation, **12P** (370 K to 629 K) lost 27.7 % of its mass while **13P** lost only 16.40 % (357 K to 641 K). The activation energy is also higher in **13P** than in **12P** in the first stage of degradation. At 773 K, the thermal stability is twice the value for **13P** than for **12P**. The above results clearly indicate the influence of linkage on thermal stability of **13P**, and it is a suitable candidate for a polymer LED.

3.9.2 Comparison of **14P** *and* **15P**

Similar to the earlier results obtained, **13P** and **14P**, in which the linkage is through the six-member ring, show higher thermal stability than **15P**, wherein the linkage is through a strained five-member ring. Unlike **13P**, at initial stages of degradation, the

mass loss and the activation energy values are comparable in both **14P** and **15P**. Above 700 K, **14P** shows greater thermal stability than **15P**. In **14P**, for a mass loss of 4.79 %, the energy required is $18.08\,\mathrm{kJ \cdot mol^{-1}}$ whereas in **15P**, for a mass loss of 16.29 %, $24\,\mathrm{kJ \cdot mol^{-1}}$ was spent for this stage of degradation. The overall results reveal that **14P** shows degradation of 32 % (335 K to 916 K) while **15P** loses 55 % in the 370 K to 863 K temperature range.

3.9.3 Comparison of **12P** *and* **4P**

Comparison of the thermal data obtained for **12P** and **4P** clearly shows the influence of electronegativity on thermal degradation. At all degradation temperatures, **12P**, which has a benzimidazole ring in the side chain, has less thermal stability than **4P** that contains a benzothiazole ring.

4 Conclusions

The overall results obtained for various thiophene polymers clearly show that the thermal stability is very much influenced by the linkage of the hetero aromatic groups, functional groups in the side chain, electronegativity of the ring, and the strain produced by the ring. Compounds like **2P**, **13P**, and **14P** show a high thermal stability compared to the other thiophene structures included in the present study. It is interesting to note that the electro-emission intensity obtained for the above polymers is also higher compared to other polymers under study. The above study helps to understand the structure–property relation in substituted thiophene, which aids in the development of novel thiophene polymers for opto-electronics.

Acknowledgment N. Somanathan thanks SFB 481 for financial support.

References

1. S. Destri, I.A. Khotina, W. Porzio, Macromolecules **31**, 1079 (1998)
2. S.C. Ng, H.S.O. Chan, P.M.L. Wong, K.L. Tan, B.T.G. Tan, Polymer **39**, 4963 (1998)
3. J.R. Sheats, D.B. Roitman, Synthetic Met. **95**, 79 (1998)
4. P. Fenter, F. Schreiber, V. Bulovic, S.R. Forrest, Chem. Phys. Lett. **277**, 521 (1997)
5. A.L. Ding, S. Pei, Y.H. Lai, W. Huang, J. Mater. Chem. **11**, 3082 (2001)
6. X. Hu, L. Xu, Polymer **41**, 9147 (2000)
7. Y. Wang, M.F. Rubner, Synthetic Met. **39**, 153 (1990)
8. G.J. Herrera, J.E. Whitten, Synthetic Met. **128**, 317 (2002)
9. C.D. Doyle, J. Appl. Poly. Sci. **5**, 285 (1961)